# Support Information

## Structural and functional analysis of human β-carotene-oxygenase 2

Linda D. Thomas, Sepalika Bandara, Vipul M. Parmar, Srinivasagan Ramkumar, Nimesh Khadka, Marcin Golczak, Philip D. Kiser and Johannes von Lintig


**Figure S1. Sequence alignment of human BCO2a, BCO2b, BCO2c and mouse BCO2.** T-coffee multiple sequence alignment was used. N-terminal leader sequence of human BCO2s are highlighted in blue. The GKAA insertion caused by a splice acceptor site polymorphism is highlighted in red. The six amino acid deletions in BCO2c is highlighted in green. Conserved active site histidine residues are highlighted in purple. Amino acid differences between human BCO2s and mBCO2 are shaded in gray.

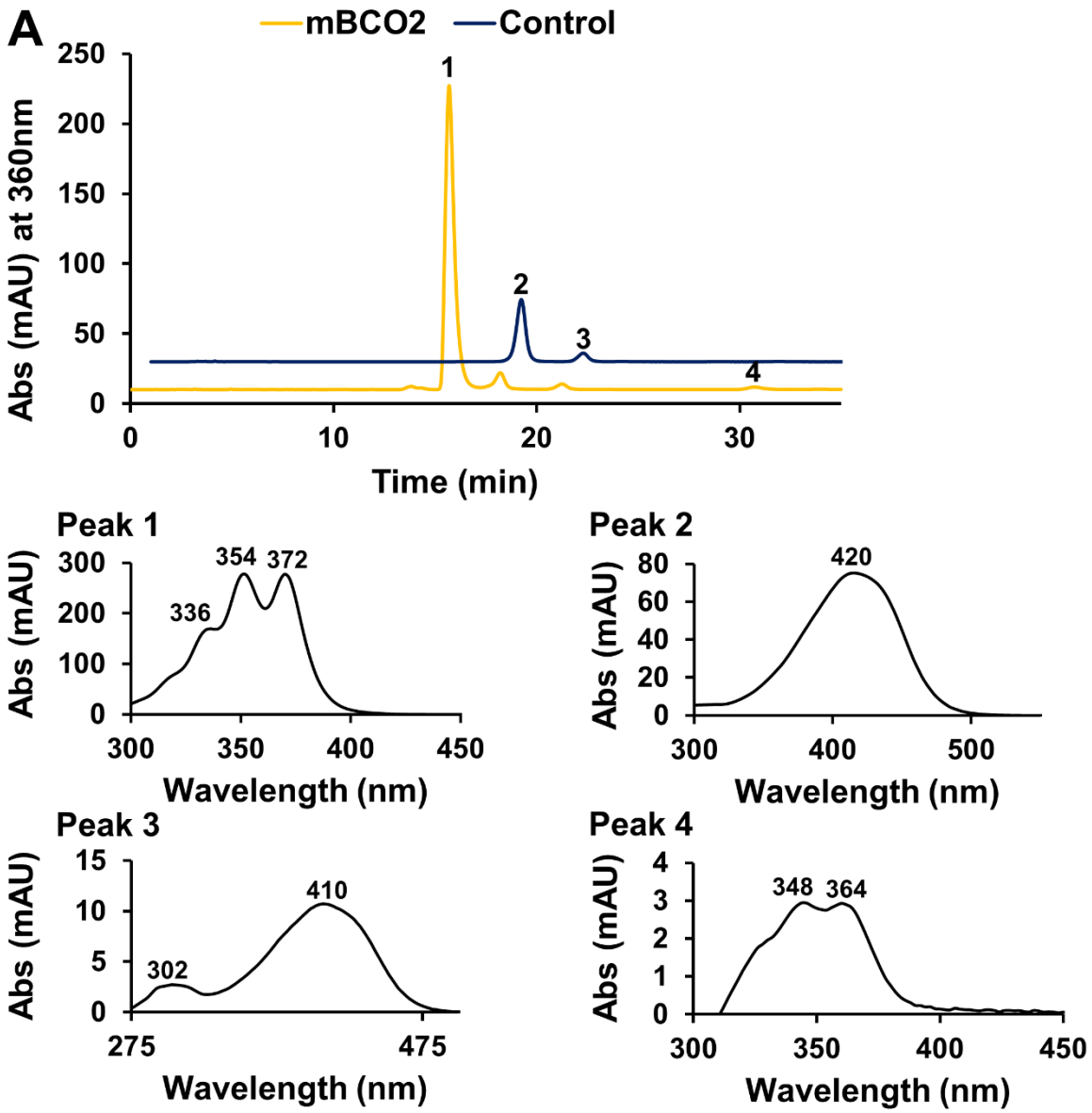


**Figure S2. mBCO2 converts apocarotenoids.** Purified (50 µg) mBCO2 (yellow trace) was incubated with substrate. Buffer incubation (navy trace) served as control. (Top panel) Representative HPLC traces at 360 nm of assays with mBCO2 (yellow) and buffer control (navy). 2000 pmol of 3-hydroxy-12'-carotenal were incubated with respective protein extracts for 12 minutes. Spectral characteristics of peak 1, 12',10-diapocarotene-12',10-dial, peak 2, 3-hydroxy-12'-carotenal; peak 3, putative *cis*-diastereomer of 3-hydroxy-12'-carotenal, and peak 4, 12',10-diapocarotene-12',10-diol are displayed in the lower panel**.**

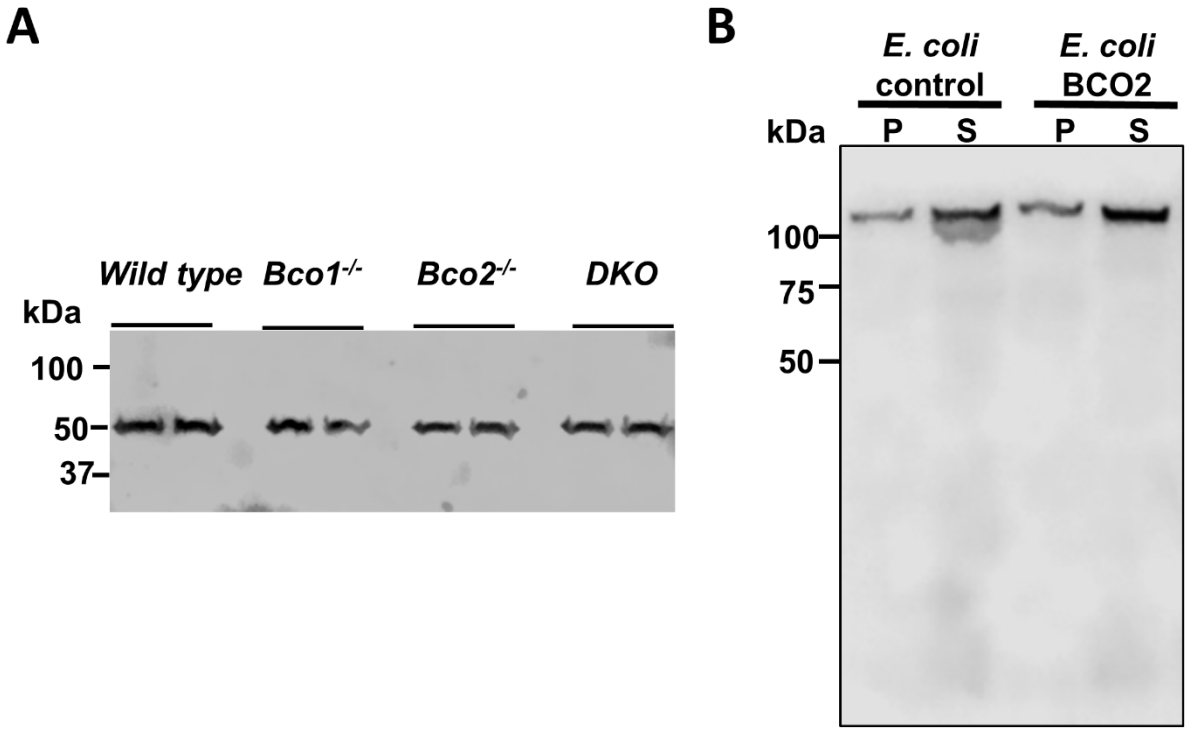


**Figure S3. Western blot analysis for human BCO2 with commercial antibody (14324-1-AP). (A)** Western blot analysis for mBCO2 in protein extracts of mouse liver using a commercial antiserum. The commercial antibody detects a protein of 50 kDa in extracts of wild type, *Bco1*$^{-/-}$, *Bco2*$^{-/-}$, and *Bco1*$^{-/-}$; *Bco2*$^{-/-}$ (DKO) mice. 30 µg of protein were separated per lane on the SDS page and each genotype was analyzed in duplicate. A band with same mobility and intensity was detected in all lanes. **(B)** *E. coli* control and *E. coli* extracts expressing human BCO2a with the commercial anti-BCO2 serum. The antibody detects a band of 110 kDa independent of the presence of BCO2 protein. Western blot was performed using cell lysate (10 µg per lane) on 10% SDS-PAGE. P, pellet and S, supernatant protein fraction.

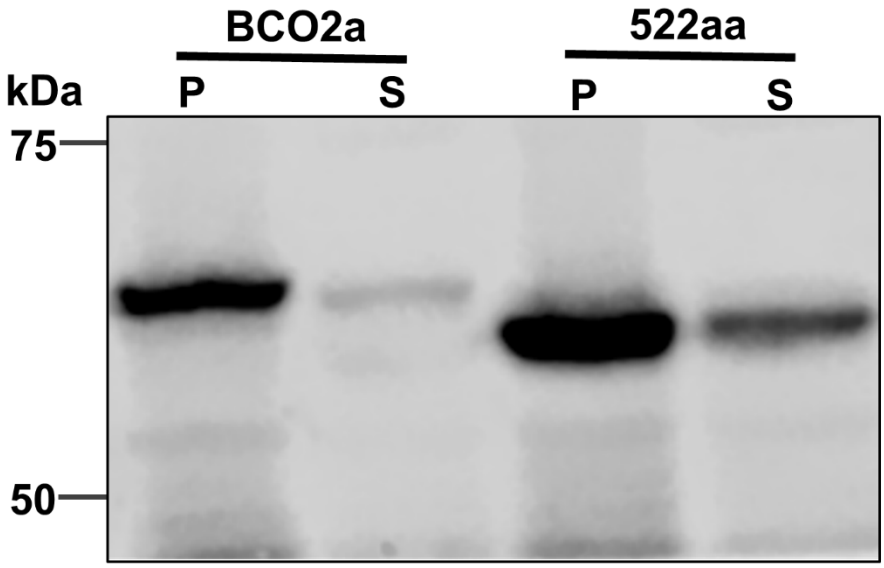


**Figure S4. Western analysis of recombinant BCO2a and truncated BCO2a (522 amino acids).** BCO2a and 522aa BCO2 were cloned into pTrcHis2-TOPO and expressed as V5-tagged in *E. coli*. Western blot was performed using cell lysate (10 µg per lane) on 6% SDS-PAGE. P, pellet and S, supernatant protein fraction.

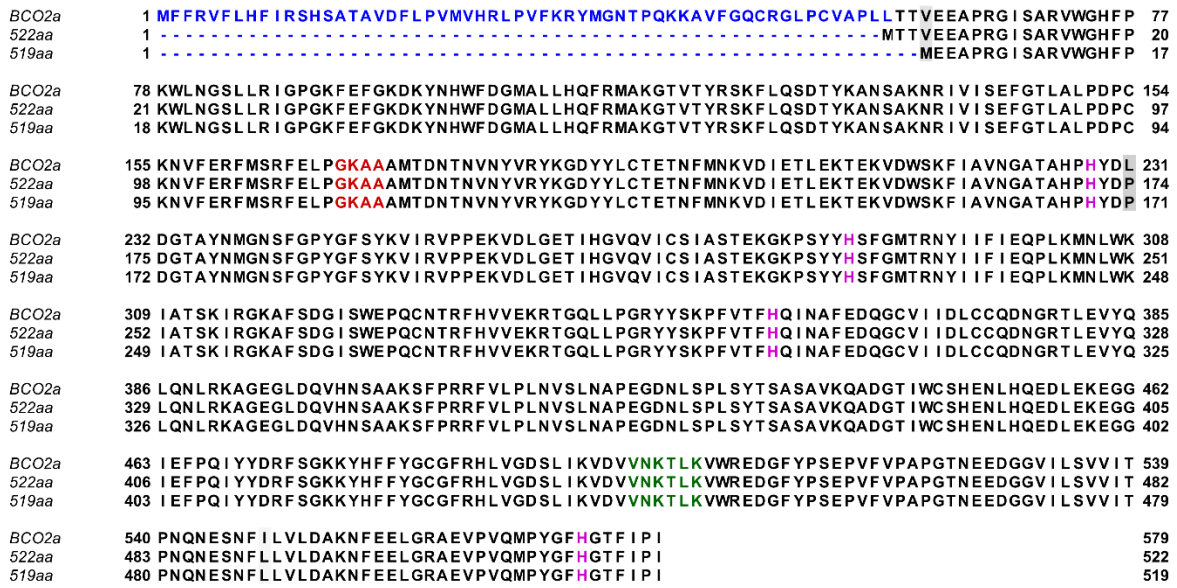


**Figure S5. Sequence alignment of human BCO2a and synthetic 522aa and 519aa human BCO2 proteins.** T-coffee multiple sequence alignment was used. N-terminal leader sequence of human BCO2a is highlighted in blue. The GKAA insertion caused by a splice acceptor site polymorphism is highlighted in red. Conserved active site histidine residues are highlighted in purple.

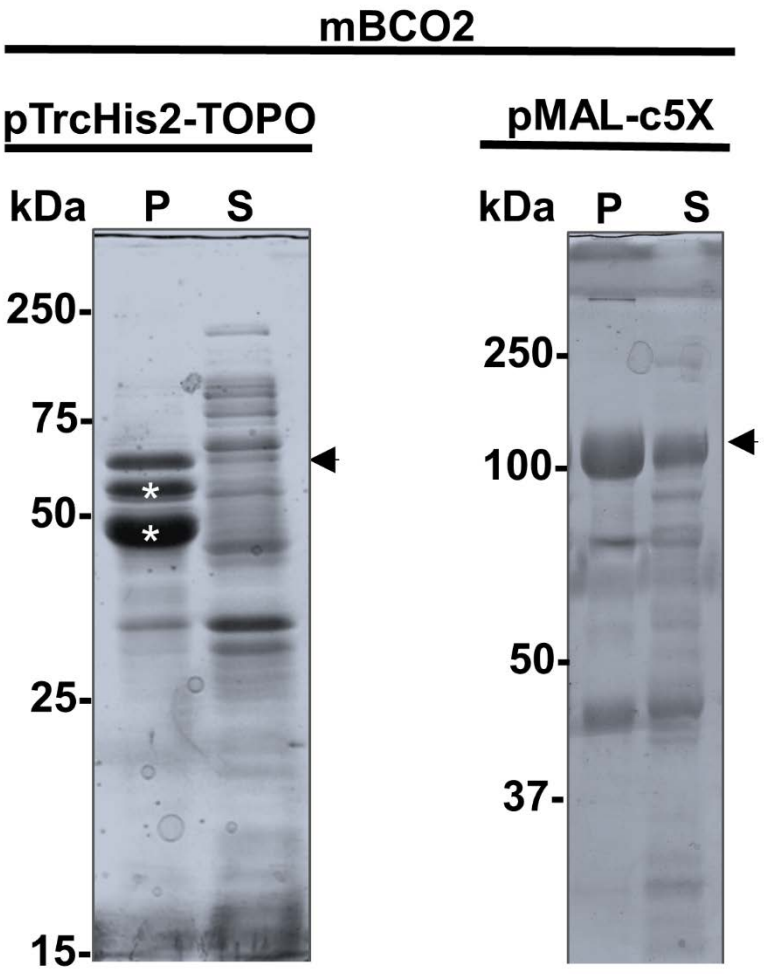


**Figure S6. SDS PAGE of mBCO2 expressed in pTrcHis2 TOPO vector and pMAL-c5x vector. (Left panel)** Coomassie blue-stained SDS-PAGE gel of protein extracts (20 µg) of *E. coli* expressing mBCO2 cloned into pTrcHis2-TOPO vector. P, pellet fraction and S, supernatant fraction. Asterisks indicated mBCO2 degradation products. **(Right panel)** Coomassie blue-stained SDS-PAGE gel of protein extracts (20 µg) of *E. coli* expressing mBCO2 cloned into pMAL-c5X expression vector. The arrow indicates the recombinant MBP-BCO2 fusion protein. P, pellet fraction and S, supernatant fractions.

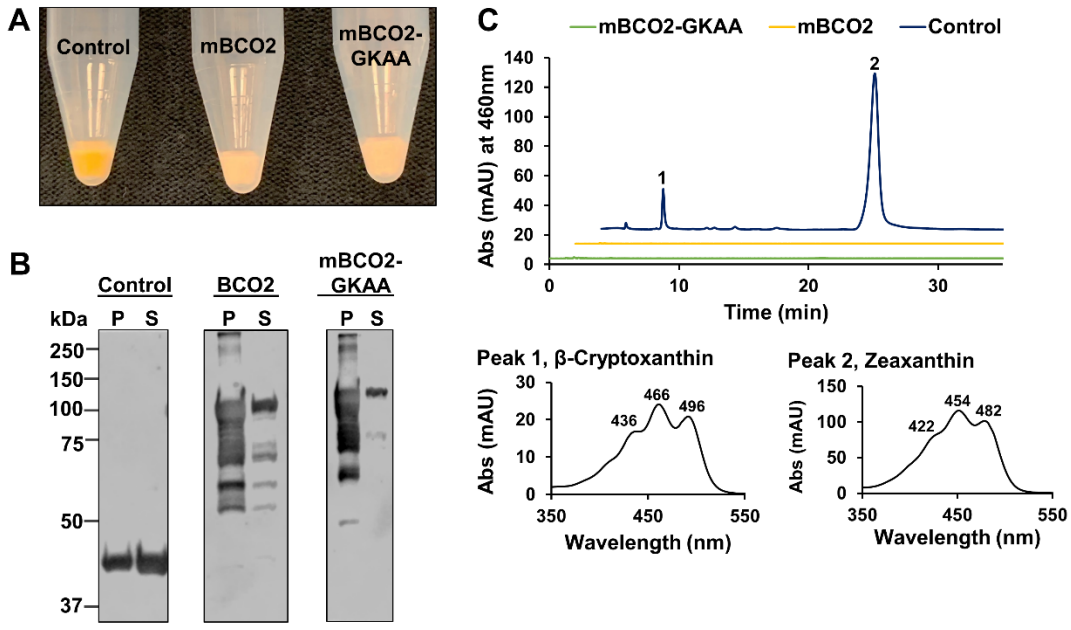


**Figure S7. The GKAA insertion does not impair mBCO2 activity.** Enzymatic activity of the mBCO2 and mBCO2-GKAA proteins expressed as maltose binding protein fusions. The vector expressing the maltose binding protein was used as control. Both mBCO2 isoforms were expressed in *E. coli* cells engineered to produce zeaxanthin. **(A)** Colors of bacteria pellets expressing maltose binding protein (control), mBCO2, and mBCO2-GKAA **(B)** Western blot of protein extracts expressing maltose binding protein (control), mBCO2, and mBCO2-GKAA. 10 µg of insoluble (P) and soluble (S) protein fraction was separated per lane. **(C)** Representative HPLC traces at 460 nm of lipid extracts from bacteria pellets expressing maltose binding protein control (navy), mBCO2 (yellow), and mBCO2-GKAA (green). Peak 1 corresponds to β-crytpoxanthin and peak 2 corresponds to zeaxanthin. Spectral characteristics of each carotenoid are displayed in the lower panel of (**C**).

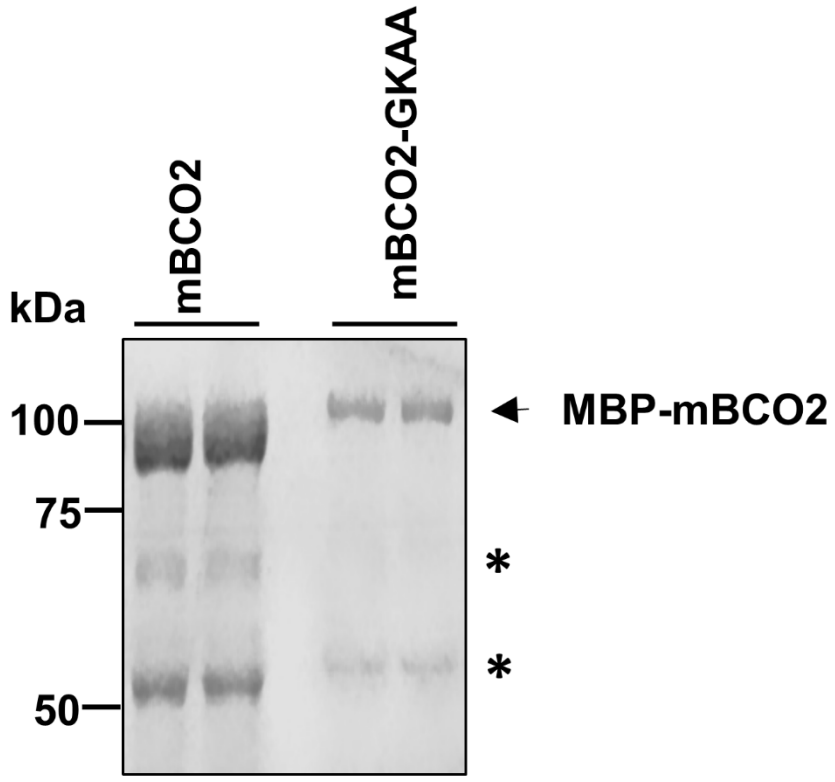


**Figure S8. SDS-PAGE of purified maltose binding protein (MBP) fusion proteins of mBCO2 and mBCO2-GKAA.** Proteins were purified by amylose affinity chromatography and purified proteins were separated on 10 % SDS-PAGE. Gels were stained with Coomassie brilliant blue g-250. The arrow identifies MBP-fusion proteins. The asterisks indicate putative degradation products/impurities.

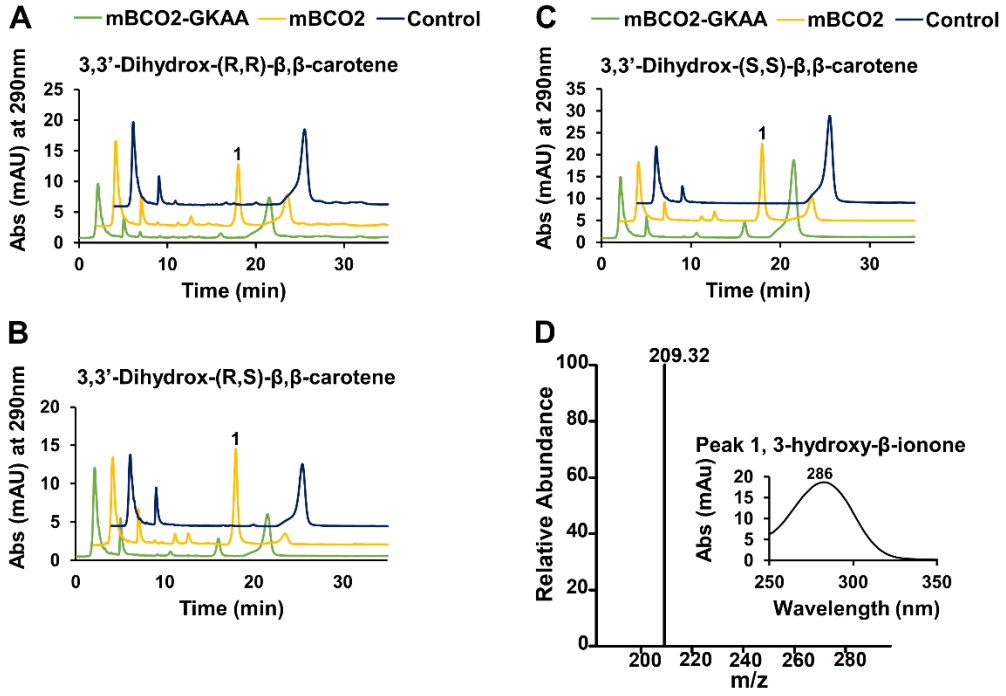


**Figure S9. HPLC traces and mass spectra of products of the conversion of zeaxanthin enantiomers by BCO2.** Purified (50 µg) mBCO2 (yellow traces) and mBCO2-GKAA (green traces) were incubated with substrate. Buffer incubations (navy traces) served as control. The reactions were carried out for 10 min. Lipids were extracted and subjected to HPLC analysis. The figure presents HPLC traces at 290 nm for the reactions with **(A)** 3(R),3(R)-β,β-carotene-diol, **(B)** 3(R),3(S)-β,β-carotene-diol, and **(C)** 3(S),3(S)-β,β-carotene-diol. **(D)** Representative spectra of peak 1, 3-hydroxy-β-ionone with corresponding representative MS-MS spectra. Note that the spectral characteristics of the 3-hydroxy-β-ionone enantiomers are identical.